Sequential Convex Programming for Collaboration of Connected and Automated Vehicles

Xiaoxue Zhang, Jun Ma, Zilong Cheng, Frank L. Lewis, *Life Fellow, IEEE,* and Tong Heng Lee

***Abstract*—This paper investigates the collaboration of multiple connected and automated vehicles (CAVs) in different scenarios. In general, the collaboration of CAVs can be formulated as a nonlinear and nonconvex model predictive control (MPC) problem. Most of the existing approaches available for utilization to solve such an optimization problem suffer from the drawback of considerable computational burden, which hinders the practical implementation in real time. This paper proposes the use of sequential convex programming (SCP), which is a powerful approach to solving the nonlinear and nonconvex MPC problem in real time. To appropriately deploy the methodology, as a first stage, SCP requires linearization and discretization when addressing the nonlinear dynamics of the system model adequately. Based on the linearization and discretization, the original MPC problem can be transformed into a quadratically constrained quadratic programming (QCQP) problem. Besides, SCP also involves convexification to handle the associated nonconvex constraints. Thus, the nonconvex QCQP can be reduced to a quadratic programming (QP) problem that can be solved rather quickly. Therefore, the computational efficiency is suitably improved despite the existence of nonlinear and nonconvex characteristics, whereby the implementation is realized in real time. Furthermore, simulation results in three different scenarios of autonomous driving are presented to validate the effectiveness and efficiency of our proposed approach.**

***Index Terms*—Autonomous driving, connected and automated vehicles (CAVs), multi-agent system, model predictive control (MPC), sequential convex programming (SCP), collaboration control.**

I. Introduction

Connected and automated vehicles (CAVs) have attracted increasing research attention in academia and industry due to their great potential to enhance the traffic safety, fuel economy, and road capacity [1]–[4]. Recent advances in communication technologies and computational resources prompt the CAVs to be crucial elements in intelligent transportation systems [5]–[7]. However, the collaboration of CAVs is still challenging due to the existence of sharing information, strong nonlinearity, and nonconvexity [8]–[12]. With the cooperation of CAVs, the decision-making process of vehicles is influenced by each other; and thus the cooperation and interaction of vehicles may naturally incur the coupling constraints that involve the decision variables of the connected (coupled) vehicles [13], [14]. The existence of coupling constraints may result in the nonconvexity and nonlinearity and increase the difficulty of achieving the cooperation task. Generally, the collaboration of CAVs can be formulated as an optimal control problem, and there are many existing methods to solve the problem and obtain the optimal solution [15]–[18].

In the existing literature, convex optimization has been a powerful tool to solve optimal control problems [19]. For convex optimization problems, there is an effective class of approaches such as linear programming (LP), quadratic programming (QP), semi-definite programming (SDP), second-order cone programming (SOCP), etc. In most cases, these convex problems can be solved in polynomial time due to their low complexity. Some of the existing algorithms, for example, the interior point method, determines an optimal solution with deterministic stopping criterion with predefined accuracy [20]–[23]. Given suitable accuracy, the optimal solution can be obtained with deterministic upper bound of the iterations. Additionally, by a self-dual embedding technique, the primal-dual interior point method can start from a self-generated feasible point, instead of the predefined initial guess. Therefore, these convex optimization methods are highly promising for the practical applications.

However, the collaboration of CAVs always leads to a nonlinear and nonconvex optimization problem, which involves the nonlinear constraints derived from the vehicles' dynamics and coupling constraints with nonconvex characteristics for collision avoidance [24], [25]. For the nonconvex optimization problem, the interior point based methods can be certainly deployed to solve the nonconvex problem; however, they are prone to be trapped into the local optimum solution and unable to realize real-time implementation for multi-agent systems. [26], [27] and [28] utilize the pseudo-spectral method to address the nonlinear system dynamics, whereas this method can not be implemented in real time, because its computational time grows dramatically with the number of agents. Another effective method is to convert the the nonconvex problem into the mixed-integer linear programming (MILP) or mixed-integer quadratic programming (MIQP) problems, which can be solved by using branch-and-cut method to obtain some feasible solutions (by decomposing the free space as multiple polytopes). Nevertheless, it will take long time if an optimal solution is required, and they also performs poorly with the number of agents increasing, even though some heuristics can be applied to accelerate the computation process [29]–[32]. In general, these methods have certain inevitable shortcomings to

X. Zhang, Z. Cheng, and T. H. Lee are with the NUS Graduate School for Integrative Sciences and Engineering, National University of Singapore, Singapore 119077 (e-mail:xiaoxuezhang@u.nus.edu; zilongcheng@u.nus.edu; eleleeth@nus.edu.sg).

J. Ma is with the Department of Mechanical Engineering, University of California, Berkeley, CA 94720 USA (e-mail: jun.ma@berkeley.edu).

F. L. Lewis is with the Automation and Robotics Research Institute, University of Texas at Arlington, Arlington, TX 76118 USA (e-mail: lewis@uta.edu).

solve the nonconvex problem. Particularly, they cannot ensure or determine a known bound of the computational time, and may not guarantee the convergence to the optimum or even a feasible point within the predefined iterations. Besides, most of them rely on the quality of the user-defined initial guess in most scenarios. Furthermore, these approaches cannot be implemented for real-time and on-board applications. Thus, it is critical to explore the use of more effective approaches to realize the deterministic convergence to the optimum in real time. Sequential convex programming (SCP) is an effective approach to solving nonlinear optimal control problem in real time. It dissects the convex problem into a sequence of convex programming problems with restricted collision-avoidance constraints, which prevents the constraints from obstruction and allows for the use of some efficient convex optimization algorithms [33], [34]. In this approach, discretizing the problem and linearizing the nonlinear constraints are required. Besides, the convexification of the nonconvex constraints is needed to make the optimization problem convex.

This paper addresses the collaborative motion planning of CAVs by using the SCP approach. The collaboration of CAVs is first formulated as a nonconvex and nonlinear model predictive control (MPC) problem in the continuous-time domain. Then the problem is discretized and linearized adequately, as the SCP requires linearization of the nonlinear optimization problem around local solutions iteratively. Besides, a quadratically constrained quadratic programming (QCQP) problem can be reformulated and convexified to facilitate the use of SCP algorithm. Thus, a sequence of simplified problems is recursively generated and solved. These simplified problems are indeed reduced to QP problems. Therefore, this approach can be applied for collaborative motion planning of CAVs rather efficiently and effectively.

The remainder of this paper is organized as follows. Section II defines the nonlinear and nonconvex optimization problem with the introduction of the dynamic model, objective function, and constraints. Section III demonstrates the problem discretization and linearization and convexification for nonconvex constraints. Section IV proposes the numerical procedures of the SCP algorithm to solve such an optimization problem. In Section V, three different scenarios in autonomous driving tasks are used to show the effectiveness and efficiency of the proposed methodology. At last, the conclusion of this work is given in Section VI.

II. Problem Formulation

A. Notation

The following notations are used in the remaining text. $\mathbb{R}^{a\times b}$ denotes the set of real matrices with a rows and b columns, $\mathbb{R}^a$ means the set of a-dimensional real column vectors. $x \succ y$ and $x \succeq y$ mean that vector x is element-wisely greater and no less than the vector y. $A^\top$ and $x^\top$ denote the transpose of the matrix A and vector x. I_a represents the a-dimensional identity matrix; $\mathbf{1}_a$ and $\mathbf{1}_{(a,b)}$ denote the a-dimensional all-one vector and the a-by-b all-one matrix, respectively; $\mathbf{0}_a$ and $\mathbf{0}_{(a,b)}$ represent the a-dimensional all-zero vector and the a-by-b all-zero matrix, respectively. The operator $\|X\|$ is the Euclidean norm of matrix X. $\otimes$ denotes the Kronecker product. $\mathrm{blockdiag}(X_1, X_2, \cdots, X_n)$ denotes a block diagonal matrix with diagonal entries $X_1, X_2, \cdots, X_n$. $\mathbb{Z}_a$ and $\mathbb{Z}_a^b$ mean the sets of positive integers $\{1, 2, \cdots, a\}$ and $\{a, a+1, \cdots, b\}$ with $a < b$, respectively. Define $\left(\{x_i\}_{\forall i\in\mathbb{Z}_1^n}\right)$ to be the concatenation of the vector x_i for all $i \in \mathbb{Z}_1^n$, i.e., $\left(\{x_i\}_{\forall i\in\mathbb{Z}_1^n}\right) = \begin{bmatrix} x_1^\top & x_2^\top & \cdots & x_n^\top \end{bmatrix}^\top$, and $\left(\{x_i\}_{\forall i\in\mathbb{Z}_1^n}\right)$ is equivalent to $(x_1, x_2, \cdots, x_n)$.

B. Network of CAVs

In order to represent the constraint or information topology of CAVs, an undirected graph $\mathcal{G}(\mathcal{V}, \mathcal{E})$ can be utilized. The node set $\mathcal{V} = \{1, 2, \cdots, N\}$ denotes the vehicles, and the edge set $\mathcal{E} = \{1, 2, \cdots, M\}$ denotes the coupling constraints (information flow) between two CAVs:

$$\begin{cases} (i,j) \in \mathcal{E}(t), & d_{\text{safe}} \le \|p_i - p_j\| \le d_{\text{cmu}} \\ (i,j) \notin \mathcal{E}(t), & \text{otherwise}, \end{cases} \tag{1}$$

where N and M are the number of vehicles and coupling constraints in the CAVs, respectively, p_i, p_j are the position vectors of the ith vehicle and jth vehicle, d_{cmu} and d_{safe} mean the maximum communication distance and minimum safe distance between two vehicles, respectively. Therefore, based on the communication topology, an adjacency matrix of the network (denoted by $\mathcal{D}$) can be obtained, which is a square symmetric matrix representing the finite undirected graph $\mathcal{G}(\mathcal{V}, \mathcal{E})$. The elements of $\mathcal{D}$ indicate whether pairs of vertices are adjacent/connected or not in the graph. Therefore, the neighbor nodes of the ith vehicle are the corresponding indexes of nonzero elements of the ith row in $\mathcal{D}$, which is denoted by $\nu(i) = \{j | (i,j) \in \mathcal{E}, \forall j \in \mathcal{V}\}$.

C. Problem Description in Continuous Time

1) Dynamic Modeling: Define the state vector as $x \in \mathbb{R}^n$ and the input vector as $u \in \mathbb{R}^m$ for vehicles. In this paper, we assume the height of the vehicle's gravity center to be zero, and neglect the pitch and roll dynamics of the vehicle. Also, we neglect the rolling resistance and aerodynamic drag. A well-known kinematic bicycle model is used to represent the vehicles' dynamics [35]. Define the state vector of a vehicle is $x(t) = (p_x(t), p_y(t), \psi(t), v(t))$ and the control input vector is $u(t) = (a(t), \delta(t))$. The system dynamics at time t is

$$\begin{aligned} \dot{p}_x(t) &= v(t)\cos(\psi(t) + \beta(t)) \\ \dot{p}_y(t) &= v(t)\sin(\psi(t) + \beta(t)) \\ \dot{\psi}(t) &= \frac{v(t)\tan(\delta(t))\cos(\beta(t))}{l_f + l_r} \\ \dot{v}(t) &= a(t) \\ \beta(t) &= \tan^{-1}\left(\frac{l_r}{l_f + l_r}\tan(\delta(t))\right), \end{aligned} \tag{2}$$

where $p_x(t)$ and $p_y(t)$ are the position of the center point of the vehicle in X and Y dimension in the Cartesian coordinates, respectively, $\psi(t)$ represents the heading angle of the vehicle in the positive X-dimension, $\beta(t)$ denotes the side slip angle between the velocity vector and the longitudinal direction of

the vehicle, $v(t)$ denotes the velocity of the vehicle, $\delta(t)$ is the steering angle, $a(t)$ is the acceleration of the vehicle, and l_f and l_r denote the distance from the front axis and rear axis to the center of gravity of the vehicle, respectively. Therefore, we have

$$\dot{x}(t) = f(x(t), u(t)), \tag{3}$$

where f denotes the dynamic characteristics of vehicles. Note that the position vector $x_p(t) \in \mathbb{R}^{n_p}$ is included in the state vector x, i.e., $x(t) = (x_p(t), \cdots)$.

2) Cost Function: Given the predicted time set $\mathcal{T} = [t_0, t_f)$ with the initial time t_0 and terminal time t_f , the cost function of the finite horizon optimal control problem for the ith vehicle is defined as

$$\min_{x_i, u_i} \int_{\mathcal{T}} \ell_i(x_i(t), u_i(t))\ \mathrm{d}t + \ell_{f,i}(x_i(t_f)), \tag{4}$$

where $\ell_i : \mathbb{R}^n \times \mathbb{R}^m \to \mathbb{R}$ is the cost-to-go regarding the states $x_i(t)$ and $u_i(t)$ at time $t \in [t_0, t_f)$, and $\ell_{f,i} : \mathbb{R}^n \to \mathbb{R}$ is the terminal cost with respect to the terminal state $x_i(t_f)$ at time t_f. In this paper, we define $\ell_i(x_i(t), u_i(t)) = \|x_i(t)\|^2_{Q_i} + \|u_i(t)\|^2_{R_i}$ where Q_i and R_i are the weighting matrices with respect to $x_i(t)$ and $u_i(t)$. Further define $\ell_{f,i}(x_i(t_f)) = \|x_i(t_f)\|^2_{P_i}$ with the terminal weighting matrix P_i.

3) Constraints: The restriction on the control input variable should be taken into consideration; hence the box constraint of the input variable is introduced as

$$\underline{u}_i \preceq u_i(t) \preceq \overline{u}_i, \tag{5}$$

where $\underline{u}_i, \overline{u}_i$ denote the minimum value and maximum value of the input variables, respectively.

Besides the box constraints, the collision avoidance constraints for the CAVs need to be satisfied as well, which gives

$$\|x_{p,i}(t) - x_{p,j}(t)\| \geq d_{\text{safe}}, \forall j \in \nu(i), \forall t \in [t_0, t_f], \tag{6}$$

where $\nu(i)$ denotes the set of neighbors of the ith vehicle and $x_{p,i}(t) \in \mathbb{R}^{n_p}$ is the position vector of the ith vehicle at time t.

Additionally, the vehicle-to-obstacle distances should also be considered in our paper. Thus, the collision avoidance constraints between vehicles and obstacles are defined as

$$\|x_{p,i}(t) - p_o(t)\| \geq d_{\text{safe}}, \forall o \in \mathcal{O}, \forall t \in [t_0, t_f], \tag{7}$$

where $p_o(t)$ is the position vector of the oth obstacle at time t, and the set $\mathcal{O}$ denotes all obstacles in the environment.

4) Problem Formulation: A finite-horizon optimal control problem can be formulated regarding the collaboration of CAVs. The objective of this problem is to calculate the optimal control inputs such that every vehicle can follow its reference trajectory without collisions. The MPC problem considers the dynamic model of the vehicles, the control input limitation, and the collision avoidance between each pair of vehicles, which can be formulated as

$$\min_{x_i, u_i} \quad \sum_{i \in \mathcal{V}} \int_{\mathcal{T}} \ell_i\left(x_i(t), u_i(t)\right)\ \mathrm{d}t + \ell_{f,i}(x_i(t_f)) \tag{8a}$$

$$\text{s.t.} \quad \dot{x}_i(t) = f(x_i(t), u_i(t)), \tag{8b}$$

$$\underline{u}_i \preceq u_i(t) \preceq \overline{u}_i, \tag{8c}$$

$$\|x_{p,i}(t) - x_{p,j}(t)\| \geq d_{\text{safe}}, \tag{8d}$$

$$\|x_{p,i}(t) - p_o(t)\| \geq d_{\text{safe}}, \tag{8e}$$

$$\forall t \in \mathcal{T}, \forall j \in \nu(i), \forall o \in \mathcal{O}, \forall i \in \mathcal{V},$$

where the terminal cost function $\ell_{f,i} : \mathbb{R}^n \to \mathbb{R}$ is $\|x_i(t_f) - x_{r,i}(t_f)\|^2_{P_i}$, and the matrix P_i is the weighting matrix for the terminal state at final time t_f.

III. Problem Reformulation and Convexification

In order to solve the problem (8) efficiently, the nonlinear and nonconvex constraints need to be discretized and convexified such that the SCP approach can be used to determine its (near-)optimal solution for the collaboration problem.

A. Discretization and Linearization

First, we need to convert the nonlinear equality constraint (8b) into a constraint that can be used in direct optimization by using a zero-order hold discretization approach. To find the numerical solution, the prediction time domain $[t_0, t_f]$ can be discretized into T equal time interval with $T+1$ nodes. The time step size $\tau_s = \frac{t_f - t_0}{T}$, and the discretized nodes are denoted as $\{t_0, t_1, \cdots, t_T\}$ with $t_{k+1} = t_k + \tau_s$. For the sake of brevity, we express $\{t_0, t_1, \cdots, t_T\}$ as the set $\mathbb{Z}_0^T = \{0, 1, \cdots, T-1\}$. Furthermore, set T as the final discrete time step $T = t_f$.

Define the state vector as $x_{i\tau} = x_i(t_\tau)$ and the input vector as $u_{i\tau} = u_i(t_\tau)$ for $x_i(t)$ and $u_i(t)$ at time $t_\tau \in [t_0, t_f)$. Then, the stacked state and control input variables can be written as $x_i = \left(\{x_{i\tau}\}_{\forall \tau \in \mathbb{Z}_1^T}\right)$ and $u_i = \left(\{u_{i\tau}\}_{\forall \tau \in \mathbb{Z}_1^T}\right)$, respectively. Since the objective of the control problem is to reduce the deviation between the real and reference trajectories as much as possible and maintain the satisfaction of collision avoidance constraints, the cost function in the MPC problem is given by

$$L_i = \sum_{\tau=1}^{T-1} \|x_{i\tau} - r_{i\tau}\|^2_{Q_i} + \sum_{\tau=0}^{T-1} \|u_{i\tau}\|^2_{R_i} + \|x_{iT} - r_{iT}\|^2_{P_i}. \tag{9}$$

In SCP, the nonlinear dynamics constraints are sequentially linearized on the nominal solutions. Given the initial nominal solution as an initial guess, the solution of the preceding iteration in SCP can be utilized for the succeeding nominal solutions. Assume the current SCP iteration is the kth iteration. Define $\hat{x}_{i\tau} = x_{i\tau}^{(k-1)}$ and $\hat{u}_{i\tau} = u_{i\tau}^{(k-1)}$ as the previous corresponding state vector and control input at the previous $(k-1)$th SCP iteration, respectively. The linearized dynamics constraints can be written as

$$x_{i(\tau+1)} = A(\hat{x}_{i\tau})x_{i\tau} + B(\hat{u}_{i\tau})u_{i\tau} - C(\hat{x}_{i\tau}, \hat{u}_{i\tau}), \tag{10}$$

where

$$A(\hat{x}_{i\tau}) = \left.\frac{\partial f}{\partial x_{i\tau}}\right|_{\hat{x}_{i\tau}, \hat{u}_{i\tau}}, \quad B(\hat{u}_{i\tau}) = \left.\frac{\partial f}{\partial u_{i\tau}}\right|_{\hat{x}_{i\tau}, \hat{u}_{i\tau}},$$

and $C(\hat{x}_{i\tau},\hat{u}_{i\tau}) = f(\hat{x}_{i\tau},\hat{u}_{i\tau}) - A(\hat{x}_{i\tau})\hat{x}_{i\tau} - B(\hat{u}_{i\tau})\hat{u}_{i\tau}$.

B. QCQP formulation

Define the vector $x_i = (x_{i1}, x_{i2}, \cdots, x_{iT}) \in \mathbb{R}^{Tn}$, the vector $x = (x_1, x_2, \cdots, x_i, \cdots, x_N) \in \mathbb{R}^{NTn}$. Similarly, we have the vector $u = \left(\{u_{i\tau}\}_{\forall\tau\in\mathbb{Z}_1^T,\forall i\in\mathcal{V}}\right) \in \mathbb{R}^{NTm}$. Given the initial state vector x_{i0} for vehicle $i \in \mathcal{V}$, we can rewrite (8) as

$$\begin{aligned}
\min \quad & \sum_{i\in\mathcal{V}} L_i \\
\text{s.t.} \quad & x_{i(\tau+1)} = A(\hat{x}_{i\tau})x_{i\tau} + B(\hat{u}_{i\tau})u_{i\tau} + C(\hat{x}_{i\tau},\hat{u}_{i\tau}), \\
& \underline{u}_i \preceq u_{i\tau} \preceq \overline{u}_i, \\
& \|x_{p,i\tau} - x_{p,j\tau}\| \geq d_{\text{safe}}, \\
& \|x_{p,i\tau} - p_{o\tau}\| \geq d_{\text{safe}}, \\
& \forall\tau \in \mathbb{Z}_0^{T-1}, \forall j \in \nu(i), \forall o \in \mathcal{O}, \forall i \in \mathcal{V}.
\end{aligned} \tag{11}$$

The nonconvex collision-avoidance optimization problem for CAVs can be intuitively formulated as a nonconvex QCQP, which can be convexified by using a convex approximation and further solved via SCP. The reason why we formulate the collision-avoidance optimization problem as a QCQP primarily lies in the characteristics of the cost function, which is usually chosen to be quadratic. Besides, quadratic inequality constraints are often used to describe collision avoidance, which means the distance among vehicles should be no less than a predefined safety distance.

Define $A(\hat{x}_{i\tau}) = \hat{A}_{i\tau}$, $B(\hat{x}_{i\tau}) = \hat{B}_{i\tau}$, $C(\hat{x}_{i\tau},\hat{u}_{i\tau}) = \hat{C}_{i\tau}$, the dynamics constraints can be rewritten as

$$x_{i(\tau+1)} = \hat{A}_{i\tau}x_{i\tau} + \hat{B}_{i\tau}u_{i\tau} + \hat{C}_{i\tau}. \tag{12}$$

The stacked state vector for the ith vehicle is represent by $x_i = \left(\{x_{i\tau}\}_{\forall\tau\in\mathbb{Z}_1^T}\right) \in \mathbb{R}^{Tn}$. Set $u_i = \left(\{u_{i\tau}\}_{\forall\tau\in\mathbb{Z}_0^{T-1}}\right) \in \mathbb{R}^{Tm}$, and then it follows that

$$x_i = \hat{\mathcal{A}}_i x_{i0} + \hat{\mathcal{B}}_i u_i + \hat{\mathcal{C}}_i, \tag{13}$$

where x_{i0} is the measured state vector at time t, $\hat{\mathcal{A}}_i \in \mathbb{R}^{Tn\times n}$, $\hat{\mathcal{B}}_i \in \mathbb{R}^{Tn\times Tm}$, and $\hat{\mathcal{C}}_i \in \mathbb{R}^{Tn}$ are given by

$$\hat{\mathcal{A}}_i = \begin{pmatrix} \hat{A}_{i0} \\ \vdots \\ \prod_{k=0}^{\tau} \hat{A}_{ik} \\ \vdots \\ \prod_{k=0}^{T-1} \hat{A}_{ik} \end{pmatrix}, \hat{\mathcal{C}}_i = \begin{pmatrix} \hat{C}_{i0} \\ \vdots \\ \sum_{s=1}^{\tau}\prod_{k=s}^{\tau} \hat{A}_{ik}\hat{C}_{i(s-1)} + \hat{C}_{i\tau} \\ \vdots \\ \sum_{s=1}^{T-1}\prod_{k=s}^{T-1} \hat{A}_{ik}\hat{C}_{i(s-1)} + \hat{C}_{i(T-1)} \end{pmatrix},$$

$$\hat{\mathcal{B}}_i = \begin{pmatrix} \hat{B}_{i0} & \cdots & 0 & \cdots & 0 \\ \vdots & \ddots & \vdots & \ddots & \vdots \\ \prod_{k=1}^{\tau} \hat{A}_{ik}\hat{B}_{i0} & \cdots & \hat{B}_{i\tau} & \cdots & 0 \\ \vdots & \ddots & \vdots & \ddots & \vdots \\ \prod_{k=1}^{T-1} \hat{A}_{ik}\hat{B}_{i0} & \cdots & \prod_{k=\tau+1}^{T-1} \hat{A}_{ik}\hat{B}_{i\tau} & \cdots & \hat{B}_{i(T-1)} \end{pmatrix}.$$

The cost function L_i for the ith vehicle can be rewritten as

$$\begin{aligned}
L_i &= \sum_{\tau=1}^{T-1} \|x_{i\tau} - r_{i\tau}\|_{Q_i}^2 + \sum_{\tau=0}^{T-1} \|u_{i\tau}\|_{R_i}^2 + \|x_{iT} - r_{iT}\|_{P_i}^2 \\
&= (x_i - r_i)^\top \hat{Q}_i (x_i - r_i) + u_i^\top \hat{R}_i u_i,
\end{aligned} \tag{14}$$

where $\hat{Q}_i = \text{blockdiag}\left(\underbrace{Q_i, \cdots, Q_i}_{T-1}, P_i\right)$ and $\hat{R}_i = I_T \otimes R_i$.

Define $u = \left(\{u_i\}_{\forall i\in\mathcal{V}}\right) \in \mathbb{R}^{NTm}$, $x_0 = \left(\{x_{i0}\}_{\forall i\in\mathcal{V}}\right) \in \mathbb{R}^{Nn}$, and $x = \left(\{x_i\}_{\forall i\in\mathcal{V}}\right) \in \mathbb{R}^{NTn}$. For all vehicles $i \in \mathcal{V}$, the total cost of all vehicles is

$$\sum_{i\in\mathcal{V}} L = (x - r)^\top \mathcal{Q}(x - r) + u^\top \mathcal{R} u, \tag{15}$$

where $r = \left(\{r_i\}_{\forall i\in\mathcal{V}}\right)$ is the concatenated reference vector for all vehicles $\forall i \in \mathcal{V}$, and the weighting matrices $\mathcal{Q} = \text{blockdiag}\left(\hat{Q}_1, \hat{Q}_2, \cdots, \hat{Q}_N\right) \in \mathbb{R}^{NTn\times NTn}$ and $\mathcal{R} = \text{blockdiag}\left(\hat{R}_1, \hat{R}_2, \cdots, \hat{R}_N\right) \in \mathbb{R}^{NTm\times NTm}$.

Concatenate the dynamics constraints for the ith vehicle (12) as the constraints for all vehicles $\forall i \in \mathcal{V}$, which can be represented by

$$x = \mathcal{A}x_0 + \mathcal{B}u + \mathcal{C}, \tag{16}$$

where $\mathcal{A} = \text{blockdiag}(\hat{\mathcal{A}}_1, \hat{\mathcal{A}}_2, \cdots, \hat{\mathcal{A}}_N) \in \mathbb{R}^{NTn\times Nn}$, $\mathcal{B} = \text{blockdiag}(\hat{\mathcal{B}}_1, \hat{\mathcal{B}}_2, \cdots, \hat{\mathcal{B}}_N) \in \mathbb{R}^{NTn\times NTm}$, and $\mathcal{C} = \left(\hat{\mathcal{C}}_1, \hat{\mathcal{C}}_2, \cdots, \hat{\mathcal{C}}_N\right) \in \mathbb{R}^{NTn}$. Substitute (16) into (15) for all vehicles, and then the total cost can be expressed as a quadratic form, denoted by

$$\sum_{i\in\mathcal{V}} L_i = u^\top \Phi_0 u + \Psi_0 u + \gamma_0, \tag{17}$$

where $\Phi_0 = \mathcal{B}^\top\mathcal{Q}\mathcal{B} + \mathcal{R}$, $\Psi_0 = 2\left(\mathcal{A}x_0 + \mathcal{C} - r\right)^\top \mathcal{Q}\mathcal{B}$, and $\gamma_0 = \left(\mathcal{A}x_0 + \mathcal{C} - r\right)^\top \mathcal{Q}\left(\mathcal{A}x_0 + \mathcal{C} - r\right)$.

The collision avoidance constraints in continuous time (6) can be rewritten in the form of discrete-time domain as

$$\begin{aligned}
& (x_{p,i\tau} - x_{p,j\tau})^\top (x_{p,i\tau} - x_{p,j\tau}) \geq d_{\text{safe}}^2, \\
& \forall i \in \mathcal{V}, \forall j \in \nu(i), \forall\tau \in \mathbb{Z}_1^T,
\end{aligned} \tag{18}$$

where $x_{p,j\tau} = \hat{\mathcal{A}}_j^{(\tau)} x_{j0} + \hat{\mathcal{B}}_j^{(\tau)} u_j + \hat{\mathcal{C}}_j^{(\tau)}$. Define the linear operator $E_{(ij)\tau} : \mathbb{R}^{NTn} \to \mathbb{R}^{n_p}$ is used to extract $x_{i\tau} - x_{j\tau}$ from x. It can be regarded as a matrix $E_{(ij)\tau} = \Big[\underbrace{\mathbf{0}_{n_p\times Tn} \quad \cdots \quad \mathbf{0}_{n_p\times Tn}}_{i-1} \quad E_{i\tau} \quad \underbrace{\mathbf{0}_{n_p\times Tn} \quad \cdots \quad \mathbf{0}_{n_p\times Tn}}_{j-i-1} - E_{j\tau} \quad \underbrace{\mathbf{0}_{n_p\times Tn} \quad \cdots \quad \mathbf{0}_{n_p\times Tn}}_{N-j-1}\Big] \in \mathbb{R}^{n_p\times NTn}$ with $E_{i\tau} = \left[\mathbf{0}_{n_p\times(\tau-1)n} \quad I_{n_p} \quad \mathbf{0}_{n_p\times((T-\tau)n-n_p)}\right] \in \mathbb{R}^{n_p\times Tn}$. Then, the vehicles-avoidance constraints (18) can be converted to

$$\begin{aligned}
& u^\top \Phi_{(ij),\tau} u + \Psi_{(ij),\tau} u + \gamma_{(ij),\tau} \leq 0, \\
& \forall i \in \mathcal{V}, \forall j \in \nu(i), \forall\tau \in \mathbb{Z}_1^T,
\end{aligned} \tag{19}$$

where the matrix $\Phi_{(ij),\tau} = -\hat{\mathcal{B}}^\top E_{(ij)\tau}^\top E_{(ij)\tau}\hat{\mathcal{B}}$, $\Psi_{(ij),\tau} = -2\left(\hat{\mathcal{A}}x_0 + \hat{\mathcal{C}}\right)^\top E_{(ij)\tau}^\top E_{(ij)\tau}\hat{\mathcal{B}}$, and the scalar $\gamma_{(ij),\tau} = d_{\text{safe}}^2 - \left(\hat{\mathcal{A}}x_0 + \hat{\mathcal{C}}\right)^\top E_{(ij)\tau}^\top E_{(ij)\tau}\left(\hat{\mathcal{A}}x_0 + \hat{\mathcal{C}}\right)$.

The collision avoidance constraints between vehicles and obstacles in the environment (7) in continuous time are equivalent to (20) in discrete time.

$$(x_{p,i\tau} - p_{o\tau})^\top (x_{p,i\tau} - p_{o\tau}) \geq d_{\text{safe}}^2, \quad \forall i \in \mathcal{V}, \forall o \in \mathcal{O}, \forall \tau \in \mathbb{Z}_1^T, \tag{20}$$

where $p_{o\tau}$ is the position vector of the oth obstacle at time stamp τ, and $x_{p,i\tau} = E_{i\tau}x$. Substituting the expression of $x_{p,i\tau}$ into (20), we can derive

$$u^\top \Phi_{(io),\tau} u + \Psi_{(io),\tau} u + \gamma_{(io),\tau} \leq 0, \quad \forall i \in \mathcal{V}, \forall o \in \mathcal{O}, \forall \tau \in \mathbb{Z}_1^T, \tag{21}$$

where $\Phi_{(io),\tau} = -\mathcal{B}^\top E_{i\tau}^\top E_{i\tau} \mathcal{B}$, $\Psi_{(io),\tau} = -2\left(E_{i\tau}\mathcal{A}x_0 + E_{i\tau}\mathcal{C} - p_{o\tau}\right)^\top E_{i\tau}\mathcal{B}$, and $\gamma_{(io),\tau} = -\left(E_{i\tau}\mathcal{A}x_0 + E_{i\tau}\mathcal{C} - p_{o\tau}\right)^\top \left(E_{i\tau}\mathcal{A}x_0 + E_{i\tau}\mathcal{C} - p_{o\tau}\right) + d_{\text{safe}}^2$.

The box constraints of control input variable for all $i \in \mathcal{V}$ can be concatenated as

$$\Psi_u u \preceq u_{\lim}, \tag{22}$$

where $\Psi_u = \begin{bmatrix} 1 \\ -1 \end{bmatrix} \otimes I_{NTm} \in \mathbb{R}^{2NTm \times NTm}$, and $u_{\lim} = \begin{bmatrix} \left(\{\mathbf{1}_T \otimes \overline{u}_i\}_{\forall i \in \mathcal{V}}\right) \\ \left(\{\mathbf{1}_T \otimes -\underline{u}_i\}_{\forall i \in \mathcal{V}}\right) \end{bmatrix} \in \mathbb{R}^{2NTm}$.

Thus, we can formulate this nonconvex programming problem in a nonconvex QCQP form, which is represented by

$$\begin{aligned} \min_u \; & u^\top \Phi_0 u + \Psi_0 u + \gamma_0 \\ \text{s.t.} \; & u^\top \Phi_{(ij),\tau} u + \Psi_{(ij),\tau} u + \gamma_{(ij),\tau} \leq 0 \\ & u^\top \Phi_{(io),\tau} u + \Psi_{(io),\tau} u + \gamma_{(io),\tau} \leq 0 \\ & \Psi_u u \preceq u_{\lim} \\ & \forall i \in \mathcal{V}, \forall j \in \nu(i), \forall o \in \mathcal{O}, \forall \tau \in \mathbb{Z}_1^T. \end{aligned} \tag{23}$$

C. Convexification

In fact, the collision-avoidance constraints (19) and (21) are concave functions, due to the fact that matrices $\Phi_{(ij),\tau}$ and $\Phi_{(io),\tau}$ in (19) and (21) are negative semidefinite. Thus, the optimization problem (23) is nonconvex and NP-hard. As the dimension of the optimization problem increases, the computational time of most known algorithms to solve a nonconvex QCQP (23) grows exponentially.

In this paper, an affine approximation is used to approximate a concave function. We know that the affine function is an upper bound on the concave function, as the concave function lies below the derived affine function at any point. Therefore, the terms $u^\top \Phi_{(ij),\tau} u$ and $u^\top \Phi_{(io),\tau} u$ in (19) and (21) can be convexified as a first-order Taylor series expansion at the operating point $\tilde{u}$, which is given by

$$\begin{aligned} &(\Psi_{(ij),\tau} + 2\tilde{u}^\top \Phi_{(ij),\tau})u + (\gamma_{(ij),\tau} - \tilde{u}^\top \Phi_{(ij),\tau}\tilde{u}) \leq 0, \\ &(\Psi_{(io),\tau} + 2\tilde{u}^\top \Phi_{(io),\tau})u + (\gamma_{(io),\tau} - \tilde{u}^\top \Phi_{(io),\tau}\tilde{u}) \leq 0, \\ &\forall i \in \mathcal{V}, \forall j \in \nu(i), \forall o \in \mathcal{O}, \forall \tau \in \mathbb{Z}_1^T. \end{aligned} \tag{24}$$

The inequalities (24) are convex with locally approximating the concave ones. Besides, the approximation is an upper bound of the original concave ones, i.e.,

$$\begin{aligned} &(\Psi_{(ij),\tau} + 2\tilde{u}^\top \Phi_{(ij),\tau})u + (\gamma_{(ij),\tau} - \tilde{u}^\top \Phi_{(ij),\tau}\tilde{u}) \\ &\geq u^\top \Phi_{(ij),\tau} u + \Psi_{(ij),\tau} u + \gamma_{(ij),\tau}, \\ &(\Psi_{(io),\tau} + 2\tilde{u}^\top \Phi_{(io),\tau})u + (\gamma_{(io),\tau} - \tilde{u}^\top \Phi_{(io),\tau}\tilde{u}) \\ &\geq u^\top \Phi_{(io),\tau} u + \Psi_{(io),\tau} u + \gamma_{(io),\tau}, \\ &\forall i \in \mathcal{V}, \forall j \in \nu(i), \forall o \in \mathcal{O}, \forall \tau \in \mathbb{Z}_1^T. \end{aligned} \tag{25}$$

Therefore, the approximated inequalities are more conservative, compared with the original concave ones. Then, the resulting problem is

$$\begin{aligned} \min_u \; & u^\top \Phi_0 u + \Psi_0 u + \gamma_0 \\ \text{s.t.} \; & (\Psi_{(ij),\tau} + 2\tilde{u}^\top \Phi_{(ij),\tau})u + (\gamma_{(ij),\tau} - \tilde{u}^\top \Phi_{(ij),\tau}\tilde{u}) \leq 0 \\ & (\Psi_{(io),\tau} + 2\tilde{u}^\top \Phi_{(io),\tau})u + (\gamma_{(io),\tau} - \tilde{u}^\top \Phi_{(io),\tau}\tilde{u}) \leq 0 \\ & \Psi_u u \preceq u_{\lim} \\ & \forall i \in \mathcal{V}, \forall j \in \nu(i), \forall o \in \mathcal{O}, \forall \tau \in \mathbb{Z}_1^T. \end{aligned} \tag{26}$$

Remark 1. In an optimization problem, restriction of the constraints can result in a smaller feasible region, a subset of the original feasible region. Thus, the minimal cost of the restricted optimization problem (26) is no less than that of the original problem. Therefore, a feasible restricted optimization problem (26) can provide a solution with a higher cost, compared with the original nonconvex optimization problem (23), which means the restricted problem (26) gives an upper bound for the nonconvex one. A solution with a lower cost will be generated by solving the problem (26) around the resulted solution iteratively for the reason that the convex inequality constraints in (26) are the upper bound of the original concave inequality constraints in (23).

IV. SCP Algorithm

Convex optimization methods are typically used to determine the global solution with predefined accuracy rather efficiently. Generally, their computational time grows polynomially along with the increase of the optimization problems' dimension and the predefined numerical accuracy for most of the convex problems. As for the nonconvex optimization methods, they may be capable of computing a locally optimal solution as efficiently as the convex optimization methods. However, it is also possible that the global solution is determined with expensive computational cost, which means their computation time has exponential growth along with the optimization problem's dimension. Here, SCP, a local optimization approach, can be used to solve the nonconvex optimization problems. Particularly, SCP aims to solve a sequence of convex optimization problems. The nonconvex optimization problem will be converted into a sequence of convex ones, each of which can be solved using convex optimization methods to obtain the global solution efficiently. The global optimum can then be obtained if SCP always converges to the same solution, given different starting points with enough amount.

Since the starting point is essential for SCP, the restricted convex program (26) may be infeasible in some cases, according to the starting point. In order to address this issue, a slack variable $\omega \in \mathbb{R}_+$ can be appended in the optimization variable u. Then, a new problem can be obtained by

$$\begin{aligned}
\min_{u,\omega} \ & \begin{bmatrix} u \\ \omega \end{bmatrix}^\top \begin{bmatrix} \Phi_0 & \mathbf{0}_{NTm\times 1} \\ \mathbf{0}_{1\times NTm} & 0 \end{bmatrix} \begin{bmatrix} u \\ \omega \end{bmatrix} + \begin{bmatrix} \Psi_0 \\ \psi_\omega \end{bmatrix} U + \gamma_0 \\
\text{s.t.} \ & \begin{bmatrix} (\Psi_{(ij),\tau} + 2\tilde{u}^\top \Phi_{(ij),\tau}) \\ -1 \end{bmatrix}^\top u + \gamma_{(ij),\tau} - \tilde{u}^\top \Phi_{(ij),\tau} \tilde{u} \le 0 \\
& \begin{bmatrix} (\Psi_{(io),\tau} + 2\tilde{u}^\top \Phi_{(io),\tau}) \\ -1 \end{bmatrix}^\top u + \gamma_{(io),\tau} - \tilde{u}^\top \Phi_{(io),\tau} \tilde{u} \le 0 \\
& \Psi_u u \preceq u_{\lim}, \ \omega > 0 \\
& \forall i \in \mathcal{V}, \forall j \in \nu(i), \forall o \in \mathcal{O}, \forall \tau \in \mathbb{Z}_1^T, \qquad (27)
\end{aligned}$$

where ψ_ω is a scalar weighting value for the additional slack variable ω.

Remark 2. A slack variable is introduced in the optimization problem (27), in order to substitute the constant trust-region size. This can increase the numerical stability during solving by guaranteeing that the solution persists to be close to the linearization operating point.

It is obvious that the problem (27) is always feasible with introducing ω. Actually, ω is related to the maximal violation of the collision-avoidance constraints under a large enough penalty ψ_ω. The violation of the collision-avoidance constraints occurs when no feasible solution to the original problem (23) can be obtained. Similar to the exact penalty method, (27) can be considered as

$$\begin{aligned}
\min_{u} \quad & u^\top \Phi_0 u + \Psi_0 u + \gamma_0 + \psi_\omega \big(\max \big(0, \\
& u^\top \Phi_{(ij),\tau} u + \Psi_{(ij),\tau} u + \gamma_{(ij),\tau}, \\
& u^\top \Phi_{(io),\tau} u + \Psi_{(io),\tau} u + \gamma_{(io),\tau} \big) \big), \\
& \forall i \in \mathcal{V}, \forall j \in \nu(i), \forall o \in \mathcal{O}, \forall \tau \in \mathbb{Z}_1^T. \qquad (28)
\end{aligned}$$

Remark 3. Since both the cost and the constraint violations are contained in (28), both the cost value and constraint violation can be reduced in this procedure.

We can use the cost value (28) to evaluate the solving process for the original problem (23). Indeed, a feasible approximated program (27) means a feasible original nonconvex problem, due to the fact that the affine approximation of a concave constraint makes the constraint more conservative, compared with the original concave one. This also indicates that if an inequality constraint in (23) is active, the corresponding inequality constraint in (27) is also active. Nevertheless, an infeasible approximated problem may not reflect that the original one is infeasible (actually, it may be feasible or infeasible). In order to overcome the infeasible nonconvex problem, the cost of the problem (28) is used for evaluation. (28) provides a measurement of the violation degree of constraints for the infeasible original problem. Define $L^{(k)}$ as the cost of the nonconvex program (23) at iteration k and $\Delta L = L^{(k)} - L^{(k+1)}$ as the reduction at iteration $k+1$. Let $\hat{L}^{(k)}$ denote the cost of the approximated program (28) at iteration k and $\Delta \hat{L} = L^{(k)} - \hat{L}^{(k+1)}$ be the reduction at iteration $k+1$. Then, $\Delta \hat{L}$ can be considered as a predicted reduction of the real reduction ΔL. Since $\hat{L}^{(k+1)}$ decreases in iterations, $L^{(k+1)}$ also decreases.

Remark 4. The computation time of SCP relies on its iteration number to convergence. As a heuristic method, SCP may fail to find an optimal solution, and the result of SCP depends on the quality of the starting point. However, in practice, SCP can always obtain a feasible solution with a lower cost.

The pseudocode of SCP is shown in Algorithm. 1.

Algorithm 1 SCP Algorithm for collaboration of CAVs at tth step.

Initialization: dynamic model for all vehicles $i \in \mathcal{V}$; communication network $\mathcal{G}(\mathcal{V}, \mathcal{E})$; parameters M, $P_{ij\tau}$; weighting matrices Q_i and R_i in the cost function; upper and lower bound of the state x and control input u, i.e., $\overline{x}, \underline{x}$ and $\overline{u}, \underline{u}$, respectively; the maximum iteration number of SCP, i.e., k_{scp}; the initial state $x_{i,0}$ at initial timestamp $\tau = 0$ for all vehicle $i \in \mathcal{V}$; the prediction horizon T; the accuracy ϵ.
Set the SCP iteration $k = 0$.
Determine the starting point $u^{(k)}$.
while $L^{(k)} - L^{(k+1)} > \epsilon$ **do**
  Evaluate the cost of the nonconvex problem $L^{(k)}$ based on $u^{(k)}$ and the constraints violations.
  Approximate the nonconvex inequality constraints based on $u^{(k)}$ by (24).
  Solve the optimal solution $u^{(k+1)}$ of the resulted convex problem (27).
  Evaluate the cost $L^{(k+1)}$ based on the computed $u^{(k+1)}$ and the constraints violations.
  $k = k + 1$.
end while

V. Numerical Validations

A. Simulation Setting

The weighting matrices in the MPC problem are set as $Q_i = I_n$, $R_i = 4000 I_m$, and $P_i = 20 I_n$. The reason why we give R_i a higher value is that the more penalty on the control input will lead to better driving comfort and smoother trajectories. Set the prediction horizon $T = 10$. The length and width of vehicles in the simulation are set to be 0.98 and 0.88 m, respectively. Set $l_f = l_r = 0.34$ m, $\tau_d = 0.03$ s, and $\tau_s = 0.01$ s. Also, set the mechanical limitation of steering angle for all vehicles are $[-3, 3]^\circ$. The length and width of all obstacles in scenario 2 are 4 and 2 m. The length and width of all the 4 obstacles in the scenario 3 are (2, 4, 4, 2) m and (4, 2, 2, 2) m, respectively. The duration of the simulation is set to be 20 s, and the MPC sampling time is 0.4 s, which means that the MPC problem will be solved every 0.4 s. Thus, the number of total steps of the simulation is 50.

Besides, the corresponding discrete reference points on the reference trajectories should be calculated to evaluate the tracking error. Here, we use the orthogonal projection of vehicle position on the reference trajectories as the first reference point. Since this point has the shortest distance to the

reference trajectories, it can obtain the fastest route to reach the reference trajectory. The remaining reference points are computed from the first reference point based on the vehicle's velocity and the sampling time of MPC.

B. Scenario 1

In this scenario, all vehicles are initially evenly distributed in a circle with a radius of 30 m. All vehicles need to go through the origin point (0, 0) m from the initial positions to the goal positions. Each different color represents a different vehicle. Set the number of vehicles $N = 8$. Fig. 1 demonstrates the trajectories of all vehicles passing through the origin in the different timestamp t, meanwhile maintaining the safe distance of 3 m. Note that t in this figure subject to $t \in \mathcal{Z}_1^{50}$. In this figure, the dotted line and solid line mean the reference trajectories and predicted trajectories in the prediction horizon. According to Fig. 1, it is evident that all vehicles can be successfully driven from the initial position to the goal position while keeping the safety distance.

As required, all vehicles' steering angle $\delta_i, \forall i \in \mathcal{V}$ should be confined into the predefined range $[-3, 3]^\circ$. For simplicity, the control input of the 1st vehicle is used to demonstrate the restrictiveness of the control inputs, as shown in Fig. 2. The black dashed lines mean the boundaries of inputs. Based on Fig. 2, the control input has been limited to the predefined range. Fig. 3 illustrates the distance among all vehicles by using different colors. The black broader solid line is to represent the safety distance. It is straightforward to observe that all the distances satisfy the collision avoidance constraints. Therefore, the effectiveness of the proposed approach in this scenario can be successfully validated.

The efficiency of the proposed algorithm is shown in Fig. 4. The computational time per optimization and per step are represented by the orange and blue line in this figure. From this figure, it is straightforward to observe that the average computational time per optimization and per step are less than 0.05 s, which renders it possible for real-time implementation.

C. Scenario 2

Assume there are some moving obstacles in the environment, as shown in Fig. 5. The gray rectangles in this figure represent the obstacles moving upwards vertically. Obviously, the real position of the vehicle will maintain the safety distance away from the moving obstacles, according to Fig. 5. Besides, the control inputs and vehicle-to-obstacle distance have also been confined into the defined ranges, as shown in Fig. 6 and Fig. 7, respectively. Moreover, the computational time per optimization and per step are shown in Fig. 8.

D. Scenario 3

In this scenario, multiple vehicles are driving in parallel and moving rightwards, as represented by different colors. There are several static obstacles located in the environment, which needs to be avoided for these vehicles. Fig. 9 presents the trajectories of 11 vehicles with avoiding the 4 obstacles

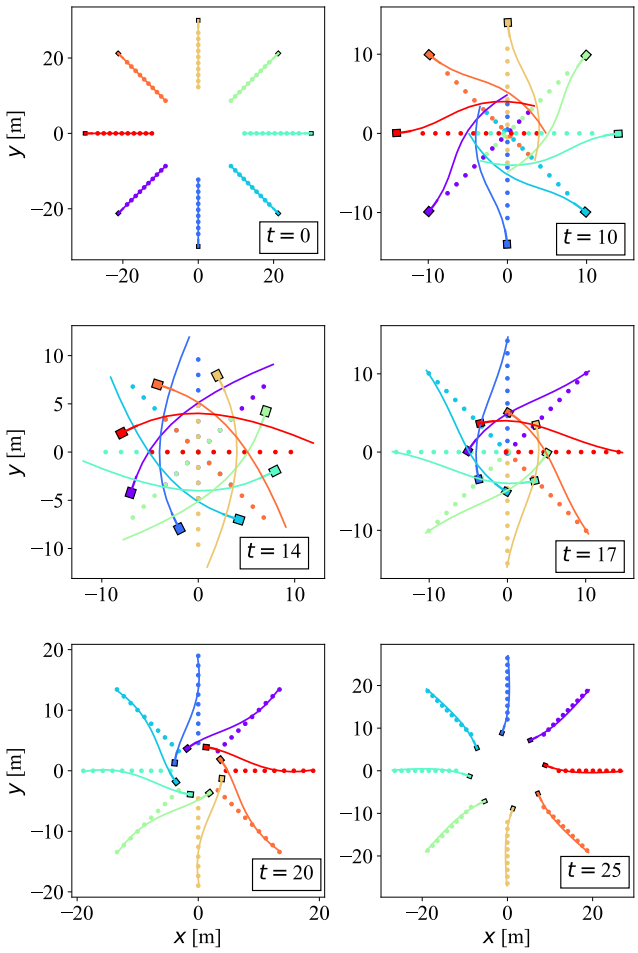

Fig. 1. Trajectories of the vehicles by using SCP in scenario 1.

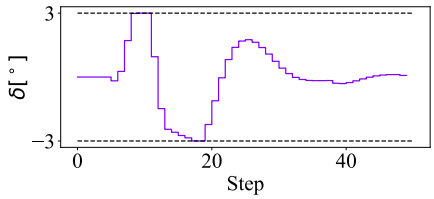

Fig. 2. Steering angle of the 1st vehicle by using SCP in scenario 1.

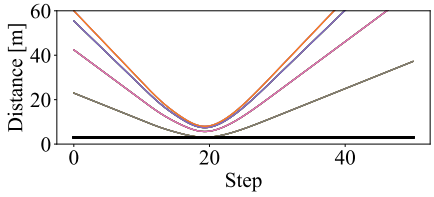

Fig. 3. Distance among all vehicles by using SCP in scenario 1. (solid lines: vehicle-to-vehicle distances; gray broader solid line: safety distance.)

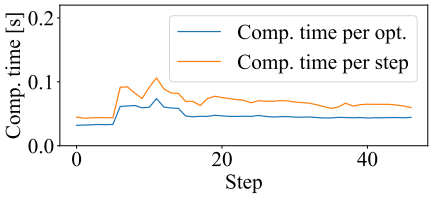

Fig. 4. Computational time spent in optimization and finishing one step by using SCP in scenario 1.

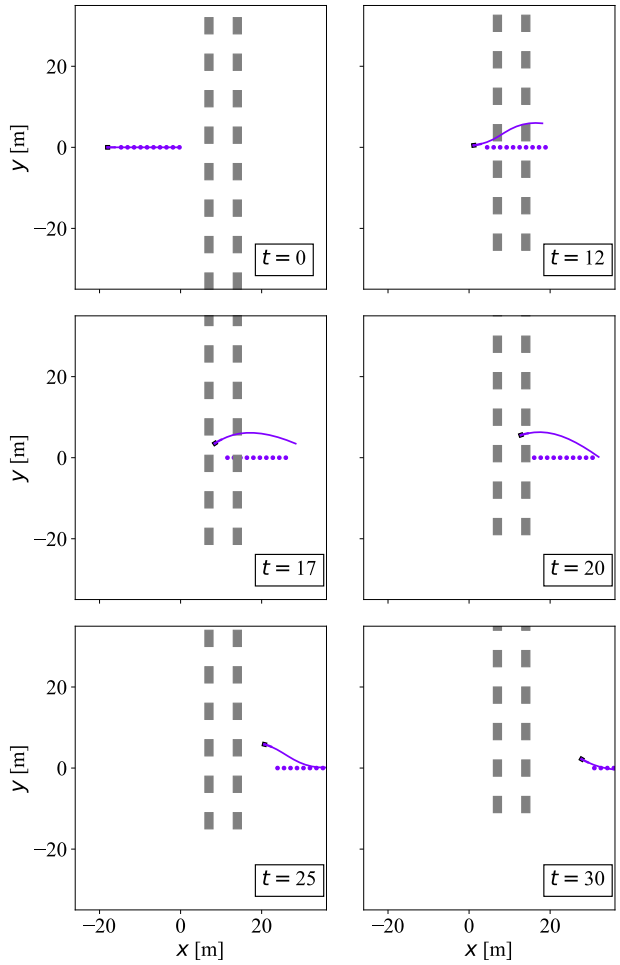

Fig. 5. Trajectories of the vehicle by using SCP in scenario 2.

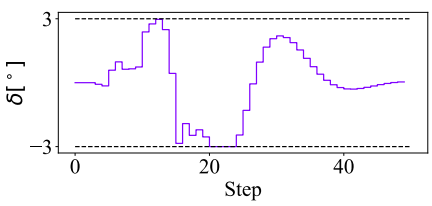

Fig. 6. Steering angle of the vehicle by using SCP in scenario 2.

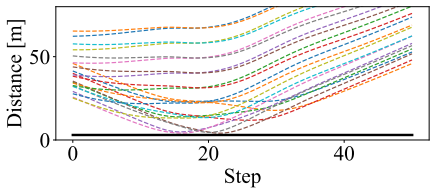

Fig. 7. Distance between the vehicle and all obstacles by using SCP in scenario 2. (dashed lines: vehicle-to-obstacle distances; gray broader solid line: safety distance.)

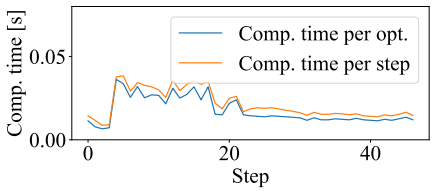

Fig. 8. Computational time spent in optimization and finishing one step by using SCP in scenario 2.

at different time. Additionally, the control input of the 1st vehicle, as an example to show the effectiveness of the proposed method, is successfully restricted into the defined range, as depicted in Fig. 10. Also, the vehicle-to-vehicle distances represented by the solid lines and the vehicle-to-obstacle distances represented by dashed lines are no less than the safety distance 3 m, as shown in Fig. 11. This also reveals the successful avoidance of the collision to other vehicles and obstacles. Similarly, the computational time per optimization and per step are displayed in Fig. 12.

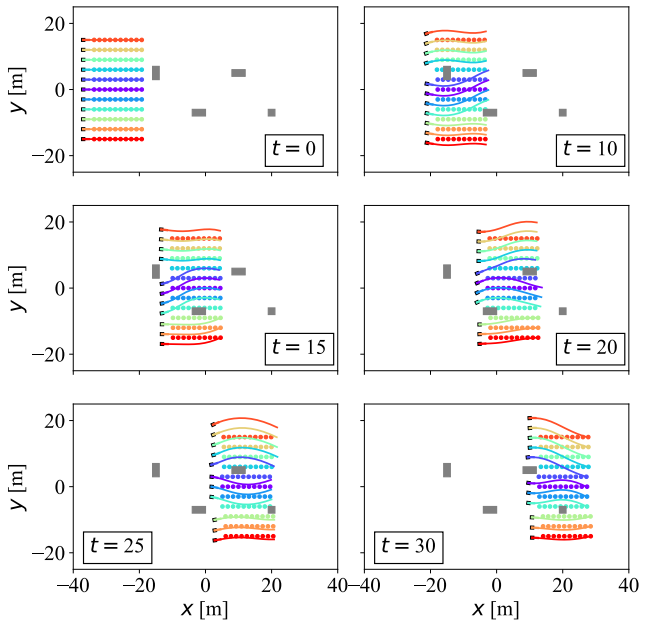

Fig. 9. Trajectories of the vehicles by using SCP in scenario 3.

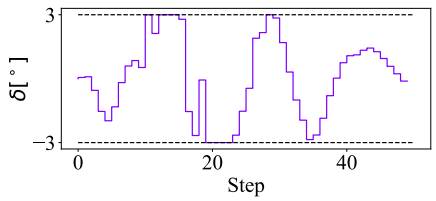

Fig. 10. Steering angle of the 1st vehicle by using SCP in scenario 3.

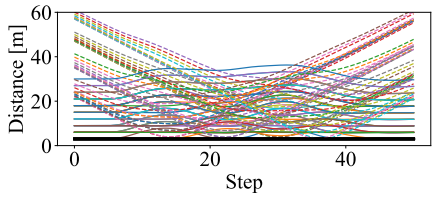

Fig. 11. Distance among all vehicles and among the vehicles and all obstacles by using SCP in scenario 3. (solid lines: vehicle-to-vehicle distances; dashed lines: vehicle-to-obstacle distances; gray broader solid line: safety distance.)

E. Comparison with MIQP

The commonly-used MIQP approach is deployed as a comparison to show the effectiveness and efficiency of the proposed approach. Here, taking the scenario 1 as an example, Fig. 13 exhibits the computational time per optimization and per step in scenario 1 with different number of vehicles ranging from $N = 3$ to $N = 20$. In this figure, the darker line shows the result of more vehicles, and the lighter line represents that of fewer vehicles. Based on this figure, the more vehicle this scenario has, the larger the problem size is, and the more time it spend.

Here, we use the scenario 1 as an example to show the effectiveness of the proposed SCP approach. Fig. 14 displays the comparison of cost values in each step with the use of SCP and MIQP in scenario 1, with different vehicle numbers. The results of varying vehicle numbers are clarified by using different colors, and the two line-styles are used to distinguish the result of SCP and MIQP. In this figure, there are some relatively higher cost values from the 5th step to the 26th step, which means there are larger deviations from the reference trajectories, due to the requirement of collision avoidance. Obviously, the more vehicles existing in scenario 1 result in a larger cost value. According to Fig. 14, we can also

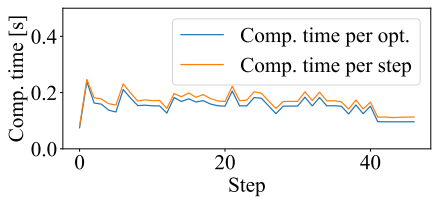

Fig. 12. Computational time spent in optimization and finishing one step by using SCP in scenario 3.

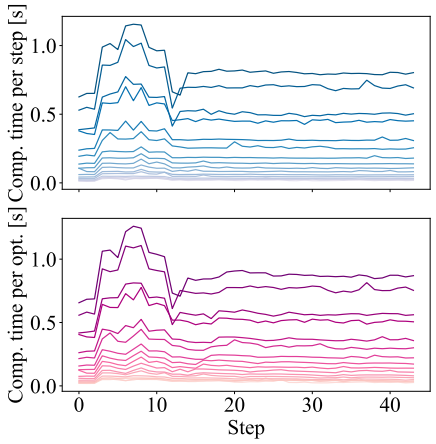

Fig. 13. Computational time spent in optimization and finishing one step by using SCP in scenario 1.

derive that the SCP approach can obtain the lower cost value, compared with the result of MIQP, which is represented by the same color with different line-styles. This also reveals the compelling effectiveness of SCP, as compared to the widely-used MIQP method.

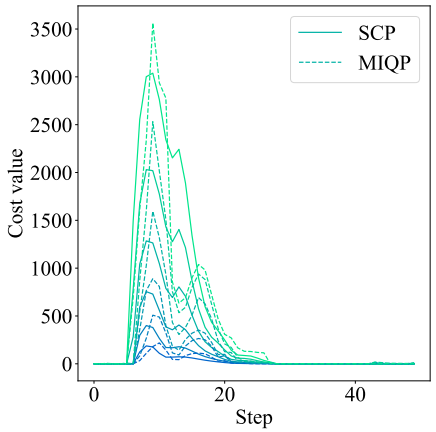

Fig. 14. Cost value by using SCP and MIQP in scenario 1.

Fig. 15 illustrates the comparison of computation time per optimization and per step by using SCP and MIQP in scenario 1 with different vehicle numbers, respectively. In this figure, the green dashed, and solid lines mean the average computational time spent in solving each optimization problem and each complete step in the MPC problem by using MIQP, respectively. Similarly, the average computational time per optimization and per step that the SCP costs are indicated by the orange dashed and solid lines. From Fig. 15, the computational time per optimization and per step of SCP are dramatically less than the computational time of MIQP, which effectively displays the efficiency of SCP. This is because MIQP is NP-complete and can be solved in exponential time and SCP can be solved in polynomial time.

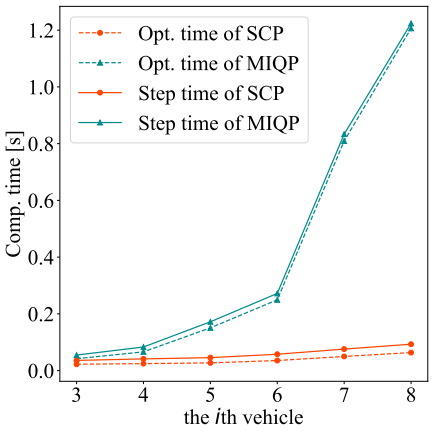

Fig. 15. Computational time spent in optimization and finishing one step by using SCP and MIQP in scenario 1.

VI. Conclusion

The collaborative motion planning problem of multiple CAVs is investigated in this paper. A general nonlinear and nonconvex MPC problem is formulated to describe the collaboration of CAVs, which requires all CAVs to finish their driving tasks and avoid potential collisions with each other as well as obstacles. Then, a real-time SCP approach is presented for the nonlinear and nonconvex MPC problem to improve the performance under nonlinear and nonconvex constraints. Hence, it facilitates the practical implementation in real time. In this method, linearization and discretization are necessary to deal with the nonlinear dynamics constraints. Also, convexification is used to address the constraints with nonconvex characteristics. At last, three different scenarios in autonomous driving tasks are considered to validate the effectiveness and efficiency of our proposed approach.

References

[1] W. Lucia, A. Venturino *et al.*, "A distributed model predictive control strategy for constrained multi-vehicle systems moving in unknown environments," *IEEE Transactions on Intelligent Vehicles*, 2020.

[2] J. K. Subosits and J. C. Gerdes, "From the racetrack to the road: Real-time trajectory replanning for autonomous driving," *IEEE Transactions on Intelligent Vehicles*, vol. 4, no. 2, pp. 309–320, 2019.

[3] S. E. Li, Y. Zheng, K. Li, Y. Wu, J. K. Hedrick, F. Gao, and H. Zhang, "Dynamical modeling and distributed control of connected and automated vehicles: Challenges and opportunities," *IEEE Intelligent Transportation Systems Magazine*, vol. 9, no. 3, pp. 46–58, 2017.

[4] Z. Wang, Y. Bian, S. E. Shladover, G. Wu, S. E. Li, and M. J. Barth, "A survey on cooperative longitudinal motion control of multiple connected and automated vehicles," *IEEE Intelligent Transportation Systems Magazine*, vol. 12, no. 1, pp. 4–24, 2019.

[5] K. Li, Y. Bian, S. E. Li, B. Xu, and J. Wang, "Distributed model predictive control of multi-vehicle systems with switching communication topologies," *Transportation Research Part C: Emerging Technologies*, vol. 118, p. 102717, 2020.

[6] B. Xu, X. J. Ban, Y. Bian, W. Li, J. Wang, S. E. Li, and K. Li, "Cooperative method of traffic signal optimization and speed control of connected vehicles at isolated intersections," *IEEE Transactions on Intelligent Transportation Systems*, vol. 20, no. 4, pp. 1390–1403, 2018.

[7] P. Hang, X. Chen, and W. Wang, "Cooperative control framework for human driver and active rear steering system to advance active safety," *IEEE Transactions on Intelligent Vehicles*, 2020.

[8] X. Zhang, J. Ma, Z. Cheng, S. Huang, C. W. de Silva, and T. H. Lee, "Accelerated hierarchical ADMM for nonconvex optimization in multi-agent decision making," *arXiv preprint arXiv:2011.00463*, 2020.

[9] P. Hang, C. Lv, C. Huang, J. Cai, Z. Hu, and Y. Xing, "An integrated framework of decision making and motion planning for autonomous vehicles considering social behaviors," *arXiv preprint arXiv:2005.11059*, 2020.

[10] P. Hang, C. Lv, Y. Xing, C. Huang, and Z. Hu, "Human-like decision making for autonomous driving: A noncooperative game theoretic approach," *IEEE Transactions on Intelligent Transportation Systems*, 2020.

[11] J. Chen, W. Zhan, and M. Tomizuka, "Autonomous driving motion planning with constrained iterative LQR," *IEEE Transactions on Intelligent Vehicles*, vol. 4, no. 2, pp. 244–254, 2019.

[12] Y. Bian, S. E. Li, W. Ren, J. Wang, K. Li, and H. Liu, "Cooperation of multiple connected vehicles at unsignalized intersections: Distributed observation, optimization, and control," *IEEE Transactions on Industrial Electronics*, 2019.

[13] S. Manzinger, C. Pek, and M. Althoff, "Using reachable sets for trajectory planning of automated vehicles," *IEEE Transactions on Intelligent Vehicles*, 2020.

[14] F. Mohseni, E. Frisk, and L. Nielsen, "Distributed cooperative mpc for autonomous driving in different traffic scenarios," *IEEE Transactions on Intelligent Vehicles*, 2020.

[15] X. Zhang, J. Ma, Z. Cheng, S. Huang, S. S. Ge, and T. H. Lee, "Trajectory generation by chance constrained nonlinear MPC with probabilistic prediction," *IEEE Transactions on Cybernetics*, 2020.

[16] J. Ji, A. Khajepour, W. W. Melek, and Y. Huang, "Path planning and tracking for vehicle collision avoidance based on model predictive control with multiconstraints," *IEEE Transactions on Vehicular Technology*, vol. 66, no. 2, pp. 952–964, 2016.

[17] X. Zhang, J. Ma, S. Huang, Z. Cheng, and T. H. Lee, "Integrated planning and control for collision-free trajectory generation in 3D environment with obstacles," in *2019 19th International Conference on Control, Automation and Systems (ICCAS)*. IEEE, 2019, pp. 974–979.

[18] J. Ma, Z. Cheng, X. Zhang, A. A. Mamun, C. W. de Silva, and T. H. Lee, "Data-driven predictive control for multi-agent decision making with chance constraints," *arXiv preprint arXiv:2011.03213*, 2020.

[19] S. Boyd, S. P. Boyd, and L. Vandenberghe, *Convex optimization*. New York: Cambridge University Press, 2004.

[20] L. E. Sokoler, A. Skajaa, G. Frison, R. Halvgaard, and J. B. Jørgensen, "A warm-started homogeneous and self-dual interior-point method for linear economic model predictive control," in *52nd IEEE Conference on Decision and Control*. IEEE, 2013, pp. 3677–3683.

[21] C. Liu, S. Lee, S. Varnhagen, and H. E. Tseng, "Path planning for autonomous vehicles using model predictive control," in *2017 IEEE Intelligent Vehicles Symposium (IV)*. IEEE, 2017, pp. 174–179.

[22] I. Necoara, D. N. Clipici, and S. Olaru, "Distributed model predictive control of leader-follower systems using an interior point method with efficient computations," in *2013 American Control Conference*. IEEE, 2013, pp. 1697–1702.

[23] J. Liu, P. Jayakumar, J. L. Stein, and T. Ersal, "A nonlinear model predictive control formulation for obstacle avoidance in high-speed autonomous ground vehicles in unstructured environments," *Vehicle System Dynamics*, vol. 56, no. 6, pp. 853–882, 2018.

[24] Z. Cheng, J. Ma, X. Zhang, F. L. Lewis, and T. H. Lee, "Neural network iLQR: A new reinforcement learning architecture," *arXiv preprint arXiv:2011.10737*, 2020.

[25] J. Ma, Z. Cheng, X. Zhang, M. Tomizuka, and T. H. Lee, "Alternating direction method of multipliers for constrained iterative LQR in autonomous driving," *arXiv preprint arXiv:2011.00462*, 2020.

[26] F. Fahroo and I. M. Ross, "Advances in pseudospectral methods for optimal control," in *AIAA Guidance, Navigation and Control Conference and Exhibit*, 2008, p. 7309.

[27] S. E. Li, S. Xu, and D. Kum, "Efficient and accurate computation of model predictive control using pseudospectral discretization," *Neurocomputing*, vol. 177, pp. 363–372, 2016.

[28] A. V. Rao, "A survey of numerical methods for optimal control," *Advances in the Astronautical Sciences*, vol. 135, no. 1, pp. 497–528, 2009.

[29] S. A. Fayazi and A. Vahidi, "Mixed-integer linear programming for optimal scheduling of autonomous vehicle intersection crossing," *IEEE Transactions on Intelligent Vehicles*, vol. 3, no. 3, pp. 287–299, 2018.

[30] A. Richards and J. P. How, "Aircraft trajectory planning with collision avoidance using mixed integer linear programming," in *Proceedings of the 2002 American Control Conference*, vol. 3. IEEE, 2002, pp. 1936–1941.

[31] A. Alonso-Ayuso, L. F. Escudero, and F. J. Martín-Campo, "Collision avoidance in air traffic management: A mixed-integer linear optimization approach," *IEEE Transactions on Intelligent Transportation Systems*, vol. 12, no. 1, pp. 47–57, 2010.
[32] C. Burger and M. Lauer, "Cooperative multiple vehicle trajectory planning using MIQP," in *2018 21st International Conference on Intelligent Transportation Systems (ITSC)*. IEEE, 2018, pp. 602–607.
[33] Z. Zhang, J. Li, and J. Wang, "Sequential convex programming for nonlinear optimal control problems in uav path planning," *Aerospace Science and Technology*, vol. 76, pp. 280–290, 2018.
[34] X. Huang and H. Peng, "Speed trajectory planning at signalized intersections using sequential convex optimization," in *2017 American Control Conference (ACC)*. IEEE, 2017, pp. 2992–2997.
[35] R. Rajamani, *Vehicle Dynamics and Control*. New York, NY, USA: Springer Science & Business Media, 2011.